Energy and Buildings 76 (2014) 597–604

Contents lists available at ScienceDirect

Energy and Buildings

journal homepage: www.elsevier.com/locate/enbuild

Indoor thermal condition in urban heat island: Comparison of the artificial neural network and regression methods prediction

Arya Ashtiani[a], Parham A. Mirzaei[b], Fariborz Haghighat[a,*]

[a] Department of Building, Civil and Environmental Engineering, Concordia University, Montreal, Canada H3G 1M8
[b] Architecture and Built Environment Department, The University of Nottingham, Nottingham NG7 2RD, UK

ARTICLE INFO

Article history:
Received 27 January 2014
Received in revised form 10 March 2014
Accepted 12 March 2014
Available online 21 March 2014

Keywords:
Urban heat island (UHI)
Heat wave
Time series regression
Artificial neural network (ANN)
Heat alert system

ABSTRACT

A side effect of urbanization, urban heat island (UHI), is well known in increases of ambient air temperature. This increase further leads to a rise in indoor environment temperature, reduction of thermal comfort, increase of cooling demand, and heat related morbidity and mortality especially among vulnerable people such as the elderlies and those living in poorly ventilated buildings. Thus, it is imperative for cities to be empowered with predictive tools during extreme heat waves in order to be able to provide emergency plans. For this purpose, it is utmost importance to develop specialized tools to predict the indoor conditions based on the outdoor conditions recorded at the weather stations. In order to develop a reliable warning system artificial neural network (ANN) and regression method were proposed and tested for an indoor air temperature forecasting application with respect to neighborhood parameters. To find the most practical approach, a cross comparison of the models was conducted by two different levels of simulation in order to present the capturing and prediction performance of the developed models. In general, the ANN model showed better accuracy in predicting the indoor dry-bulb temperature while it was more complicated in implementation.

1. Introduction

Industrial revolution between 1760 and 1840 demanded a massive population as labors to be settled within urban areas. The rush behind this mass settlement resulted in an unplanned urbanization lasted until the recent era. The urban to rural population gradually increased from less than 10% in 1800 to less than 30% at the end of Second World War, 1945. Due to various socio-economic reasons urbanization had even a higher growth slope from less than 30% to about 50% between the Second World War and the recent time. During these years cities experienced significantly higher temperatures than their nearby rural areas [1]. This phenomenon, known as urban heat island (UHI), has been broadly investigated and documented in many cities, i.e. London [2], Montreal Island [3], Toulouse [4], Mediterranean cities [5], Mexico [6], Atlanta [7], and Hong Kong [8].

The undesired side effects of UHI on decreasing outdoor air quality, increasing air conditioning energy consumption, heat related illness and mortality are among the motives to study its influential parameters, mitigation strategies and prediction methods. UHI is mainly intensified during heat waves which are reported to be more frequent in the recent years. Hajat et al. [9] defined heat wave as a three day rolling average above the 97th percentile value of 21.5 °C. Heat waves are ranked first as the cause of human mortality compared to other meteorological hazards, i.e. floods, hurricanes, and tornadoes while they poses threats to property and human health [10]. The National Weather Service Office of Climate, Water, and Weather Services estimated that a total of 2248 people throughout the United States lost their lives due to extreme heat waves between 1986 and 2000. Moreover, a loss of 2200 million dollars was estimated due to the extreme heat weather during the same period [10]. The death of around 50,000 people in heat wave of August 2003, in Europe is the recent example of an intensified heat island [1].

The frequency and severity of extreme weather events and heat waves are projected to increase as a result of climate change. Meanwhile, the global warming trends are projected to double the likelihood of such events [11]. Further projections suggest a heat wave of similar magnitude of summer 2003 may occur as frequently as every three years by the 2050s [12–14]. Considering the growing numbers of vulnerable people (e.g. elderly and children) and increasing social isolation, significant number of people will be susceptible to heat wave-intensified heat islands. Thus, establishment of heat watch-warning systems and mitigation plans is necessary in order to protect the public and especially vulnerable habitants.

* Corresponding author.
E-mail address: Fariborz.Haghighat@Concordia.ca (F. Haghighat).

http://dx.doi.org/10.1016/j.enbuild.2014.03.018
0378-7788/

In many cities, the primary heat alert systems were based on the computation of the outdoor temperature and heat index [15,16]. However, the dynamic interaction between building and external climate is extremely complex, including a large number of complicated variables and phenomena. The fact that the human body responds to the total effect of all-weather variables interacting simultaneously on it, rather than to individual meteorological elements, encourages researchers to design more effective heat watch-warning systems; obviously, a better emergency plan leads to an improvement in human health survival by reducing the number of morbidity and mortality. One should add that the vulnerable groups of people mainly spend more time in their places than outside during a heat wave day [17]. Thus, the predicting indoor thermal conditions rather than that of the outdoor thermal condition helps city planners to provide better emergency plans for vulnerable people. This means that the development of a heat alert system based on the indoor thermal conditions is highly preferred.

To date, there are limited studies that have been carried out to explore the use of different statistical and numerical methods in predicting indoor air condition during intensified UHI with the heat wave. As one of the major drawback, the complex interaction between outdoor and indoor is barely resolved while various building simulation programs are mainly decoupled from non-isothermal airflow passing over the buildings' surfaces [18]. On the other hand, outdoor models barely consider the indoor interactions inside a building (i.e. generated and stored heat) where it is assumed as an isolated objects in such models. Hence, to link the complex interaction between indoor and outdoor environments, the statistical methods have the advantages of being simpler and faster in the prediction applications. The traditional models are mainly driven based on the regression approach [19]. With emerging more advanced techniques such as the artificial neural network (ANN), however, more accurate prediction is expected.

Regression models have been widely used for the predicting and forecasting purposes [20]. In regression analysis, a linear or non-linear correlation between a dependent variable and one or more independent variables is assumed. The distant observations from the rest of data can have huge effects on the linear regression by decreasing the accuracy of the prediction since extreme values cannot be always captured in the predictions.

Artificial neural networks (ANNs) are known as effective method for approximating non-linear model function. Considering the

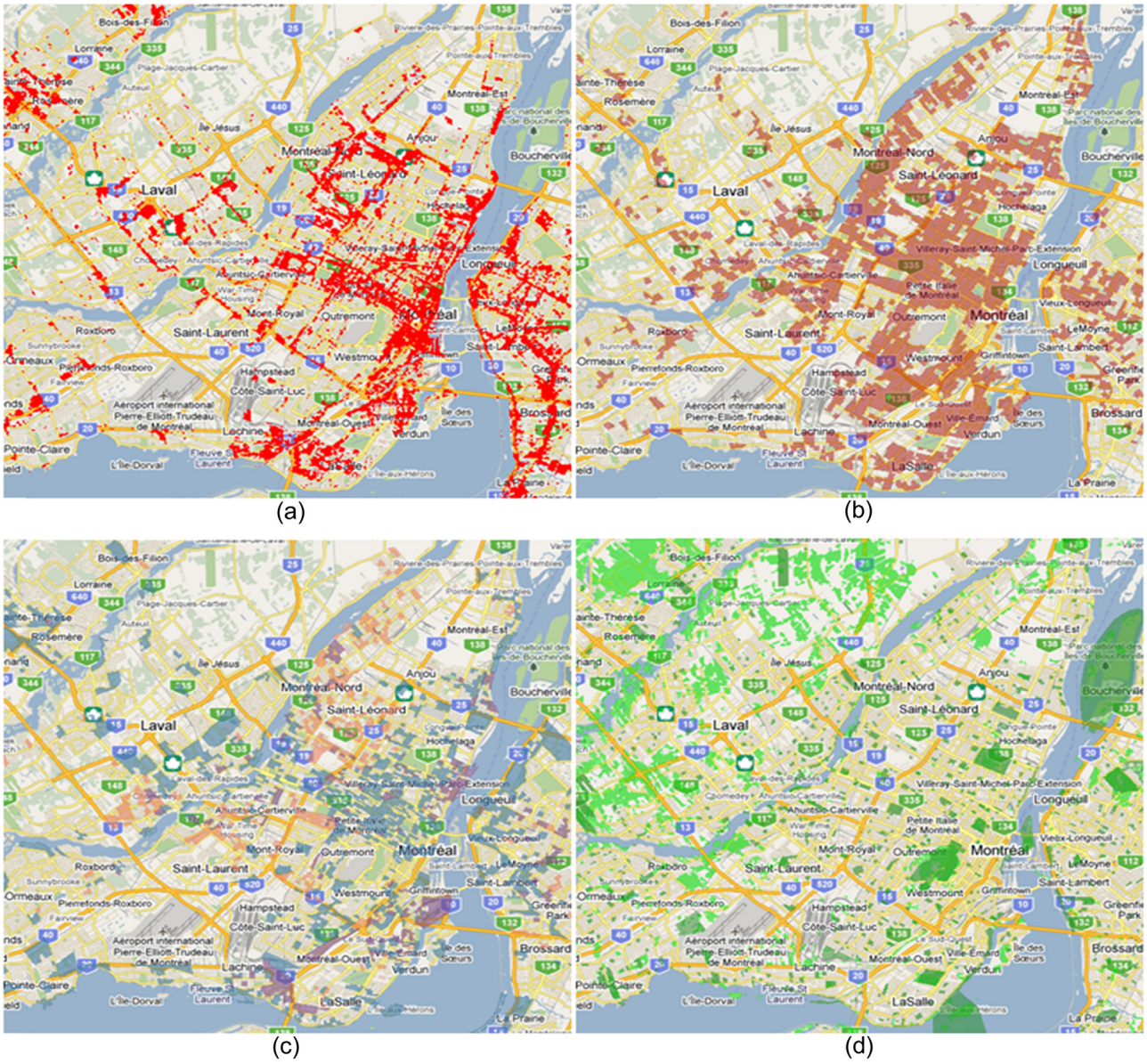

Fig. 1. (a) High surface temperatures, (b) high population density, (c) socio-economically deprived areas, and (d) minimal vegetation.

highly non-linear relation between the outdoor environment (air temperature, solar radiation, wind speed, etc.) and the indoor air temperature, the ANNs method can be an efficient way to find the relation [21–25]. Thomas and Soleimani-Mohseni [26] discussed on how to identify black-box indoor air temperature prediction models in buildings. Their measured data include internal heat power, indoor air temperature, outdoor air temperature, solar radiation, and time of the day for six days every 10 min. Different linear and nonlinear prediction models were identified and compared. As another example, [27] adapted ANN to predict the indoor air temperature and relative humidity in a house where indoor and outdoor temperature and relative humidity were measured every 15 min for 30 days.

The main objective of this paper is to perform a cross comparison study between a traditional and an advanced heat warning model: regression and artificial neural network (ANN). These models are expected to predict the indoor air thermal condition in buildings occupied by most vulnerable people with low income living in hot and highly populated areas. A field measurement dataset, carried out in Montreal during the summer of 2010, was used to develop and train the abovementioned models.

2. Measurement

Meteorological data were obtained from the Pierre-Elliot Trudeau airport weather station, Montreal, Canada. Four variables were measured in an hourly basis, including outdoor dry-bulb temperature, wind speed, solar radiation, and relative humidity. In order to identify the vulnerable regions, first, satellite thermal images were utilized to characterize Montreal urban areas and zones with high surface temperature in summer. Then, 'Urban Heat Island Mapping Tool' prepared by '*ICU – INSPQ et DSP de Montreal* was used to evaluate and choose potential zones for recruiting potential buildings. This tool made it possible to locate the most thermally vulnerable areas against UHI in Montreal Island by considering four additional influential factors: (1) areas determined to have the highest surface temperatures with a minimum density of 400 inhabitants per km^2 (Fig. 1(a)), (2) areas with population density more than 5001 people per km^2 (Fig. 1(b)), (3) areas included deprived occupants who cannot afford air conditioning (Fig. 1(c)), and (4) areas located far from vegetation or with low vegetation ratio (Fig. 1(d)) [28]. Finally, 55 residential buildings were identified on the Island of Montreal. A measurement campaign was conducted to monitor the indoor thermal characteristics (i.e. dry-bulb temperature) of these 55 residential buildings (for more details see [30]).

The indoor thermal characteristic of the selected buildings are influenced by the outdoor weather, the building occupants' behavior and the surroundings. The neighboring characteristics of each building clarify the link between these temperatures. In order to account the neighboring effect at the same time with building envelope characteristics (e.g. albedo and thermal capacity), the studied buildings were further divided into four major groups:

a) top floor dwellings located in downtown Montreal,
b) other dwellings located in downtown Montreal,
c) top floor dwellings located in other sample areas, and
d) other dwellings located in other sample areas.

3. Methodology

3.1. Influential parameters

A traditional regression method in addition to an advanced ANN model was developed to perform a cross-comparison study. In the development of regression method, the relationship between one or more independents, predictors, or repressor variables and a dependent or criterion is considered in such a way to make the sum of square residuals of the model minimum. In statistics, time series analysis is the study of data collected in a certain period of time to determine an outcome in relation to its history. All these data are taken at different times, but spaced in the same time interval. Time series analysis comprises methods for analyzing time series data in order to extract meaningful statistics. In fact, time series forecasting is the use of a model to predict future values based on previously observed values. The following equation represents a simple exponential smoothing time series, which is well known as autoregressive model (AR) and was used in this study:

$$T_i(t) = a_0 + a_1 T_e(t) + a_2 T_e(t-1) + \cdots + a_p T_e(t-p) + bW(t) + cRH(t) + d \quad (1)$$

where a_i, b, c and d are the coefficients. $T_i(t)$ is the indoor dry-bulb temperature measured at time t. $T_e(t)$ represents the sol-air temperature calculated at time t, based on the outdoor dry-bulb temperature and direct normal solar radiation. $W(t)$ represents the wind speed. $RH(t)$ is the relative humidity.

On the other hand, the ANN model is a data-driven process since the analysis and the results depend on the available data. It has the ability of approximation of arbitrary and complex non-linear relationship between the large input and output datasets whose analytical forms are difficult or impossible to be obtained.

To provide suitable dataset for both models, first the influential parameters, which have significant role in the UHI formation and intensification, have to be identified. These parameters are extensively discussed in literatures associated with formation of heat island or trapping and storing heat inside the urban canopies. The mentioned parameters have been included in development of both regression and ANN models, which are discussed in the following sections.

3.1.1. Outdoor dry-bulb temperature

It is well established that outdoor dry-bulb temperature has significant influence on the indoor environment thermal condition. For example, [17] has highlighted the outdoor dry-bulb temperature as an important parameter.

3.1.2. Solar gain

Solar radiation contributes in the formation of diurnal UHI due to the ability of urban surfaces in trapping radiation and storing heat, especially during the clear sky [29,30]. In this study, the solar radiation was estimated with the percentage gains of direct normal solar radiation on the building by every assembly. First, direct normal solar radiation data were collected on an hourly basis throughout the months of June, July, and August 2010 at Pierre-Elliot Trudeau International Airport. Then, the total diffuse radiation on vertical surfaces, I_d, was calculated [31]:

$$I_d = I_{DN} \times [C \times F_{ss} + 0.5\rho_g(C + \sin\ \beta)] \quad (2)$$

where I_{DN} is the direct normal solar radiation, C, the diffuse radiation factor, F_{ss}, the angle factor between vertical surface and the sky, ρ_g, the ground reflectance, and β the solar altitude angle. First, the solar heat gain per area of each building assembly (roof, wall, and window) was calculated. Based on the heat gain per area of assemblies, the percentage gains of direct normal solar radiation on the building for every assembly were calculated. Evidently, these values are almost constant for each assembly regardless of the location of the building. In case of top floor units (detached), by considering both horizontal and vertical surfaces, it was calculated that about 65% of direct normal solar radiation was absorbed by assemblies while for the rest of floors in the sample study, these values were calculated about 14% (Table 1).

3.1.3. Sol-air concept

In this study, the sol-air temperature was used to include the simultaneous effect of the solar radiation and outdoor ambient temperatures. Starting from morning, the solar gain tends to gradually increases to a maximum value at noon while it starts to gradually decrease to zero at sunset. It should be mentioned that the regression methods are weak in accurately combining the effect of solar radiation and outdoor dry-bulb temperature. In other words, the frequencies of appearance of zero values (during night) for solar radiation and their differences with other non-zero values make the regression models unable to accurately predict the indoor air temperature. Therefore, the sol-air temperature concept employed to enhance the accuracy. Moreover, using sol-air temperature reduces the number of input variables for each method and simplifies the analysis. The following formula represents the employed sol-air temperature:

$$T_e = T_o + \frac{\alpha I_t}{h_o} - \frac{\varepsilon \Delta R}{h_o} \tag{3}$$

where T_e is the sol-air temperature, I_t is the incident solar radiation, and h_o is the assigned surface conductance. The combined coefficient h_o is equal to the sum of the convection and radiation coefficients. The value of h_o is subjected to substantial variation with both temperature and wind speed over the surface, but a value of 23 W/m^2. $^\circ$C is commonly used. The value of the emittance, ε, is assumed to be 1. ΔR is defined to present the difference between the incident long-wave radiation (from the sky and surroundings) and the ideal radiation emitted by a blackbody at outdoor air temperature. The value of ΔR is approximated about 60 W/m^2 for the horizontal surfaces while it is assumed to be $\Delta R = 0$ for the vertical surfaces. α is the absorptance of the studied buildings.

3.1.4. Local wind speed

Lam [32] stated that the constructed buildings increase the roughness of the surface underlying of the atmosphere resulting in a wind speed decrease near the ground. Air movement over the building surface affects the convective heat transfer at the building surface, which is an important factor in heat transmission through the building enclosure, surface temperature, and cooling rates. The impact of surface roughness in the approaching wind was modeled using the power law [31]:

$$\frac{V_z}{V_g} = \left[\frac{Z}{Z_g}\right]^{\theta} \tag{4}$$

where Z is the height of the buildings under study. The mean speed exponent (θ) corresponds to the terrain category over which the under studied buildings and the airport are located. V_z is the mean speed at specified height. V_g and Z_g are the gradient speed and height, respectively. Two different wind speed profiles were considered for the studied cases in Montreal Island; one for the downtown area, and one for the other studied areas.

3.1.5. Relative humidity

In addition to dry bulb temperature, relative humidity is considered in many models as one of the influential parameters in the formation of UHI [29,33]. For example, an inverse relationship between moisture and nocturnal UHI was reported by [34].

3.1.6. Time of the day

Gobakis et al. [35] emphasized on the importance of this parameter in their studies. Mirzaei et al. [30] claimed that integrating of the day time would improve the performance of the ANN model due to the temporal variation of the contributing parameters (i.e. wind and relative humidity).

3.1.7. Location of the measured indoor temperature

The natural tendency of warmer air to move upward in the buildings was accounted as a major parameter in this study. Residences on the top floors of buildings are at a greater risk of overheating, heat related illnesses, and deaths due to the buoyancy effects mainly in the poorly ventilated building [36].

3.1.8. Vegetation ratio

Lower temperatures are always assigned to the green areas compared to the high-density areas in a metropolitan. In other words, replacing vegetation with built-up areas leads to having a warmer temperature in these areas in comparison with suburbs [37].

3.1.9. Urban and building geometry

Ambient air temperature within a street canyon depends on the wind speed and velocity profile inside that canyon. Aspect ratio, the ratio of building height to the distance between adjacent buildings, significantly affects the wind velocity profile within a street canyon [1]. This parameter was selected as a representative of the urban and building geometry in this study.

3.1.10. Occupancy

Another dominant parameter on the increases of the indoor dry bulb temperature is the generated heat within the building due to the occupants' pattern of activities [11].

3.1.11. Building volume

The total building volume is assumed to be proportional to the building thermal mass. This implies that a building with a higher thermal mass has more capacity to store energy [30]. Wright et al. [38] also stated since buildings have thermal mass, the history of outdoor air temperature over a few days should be taken into consideration in order to analyze the indoor air temperature.Table 1 summarizes some of the parameters used in the simulation.

3.2. Input data processing

As mentioned earlier, four different categories of building unit groups were defined as the dataset. To develop the regression and ANN models and to find the worst case scenario of the indoor dry-bulb temperature, which is the target of this study, the obtained information, assumptions, and neighborhood measurements are further summarized in Table 2.

As shown in Table 2, categories (a) and (b) are located in downtown Montreal, however, the location of the sensor is the only variable. This number (sensor location) is allocated one for the top units and zero for other floor. The exposed surface area of the façade is higher in top units, which implies a higher amount of solar gain for the top unit. Therefore, the only variable parameter in all the dwellings located in downtown Montreal is the solar gain; it would be hence reasonable to consider the top floor units as the candidate for the worst thermal case scenario or the target study places in this area. Similar arguments can be made for the dwellings located in other areas (categories (c) and (d)). Thus, these locations again can be considered as the potential candidate as the target study places.

Furthermore, to find the worst case scenario between two categories (a) and (c), their other influential parameters were further compared together. Due to higher aspect ratio, volume height and lower vegetation ratio, it can be concluded that the top roof units located in downtown buildings have the worst indoor thermal condition during the heat waves, and thus should be chosen as the target buildings for the model development. This conclusion is clearly supported by the measured indoor dry-bulb temperatures campaign.

Table 1
Coefficients used in 3.1.1 to 3.1.11.

β (%)		h_0 (W/m^2 °C)	ε	ΔR (W/m^2)		Mean speed exponent (θ)		Z_g (m)	
Top floor units	Other			Horizontal surfaces	Vertical surfaces	Downtown	Other	Downtown	Other
65	14	23	1	60	0	0.36	0.25	500	400

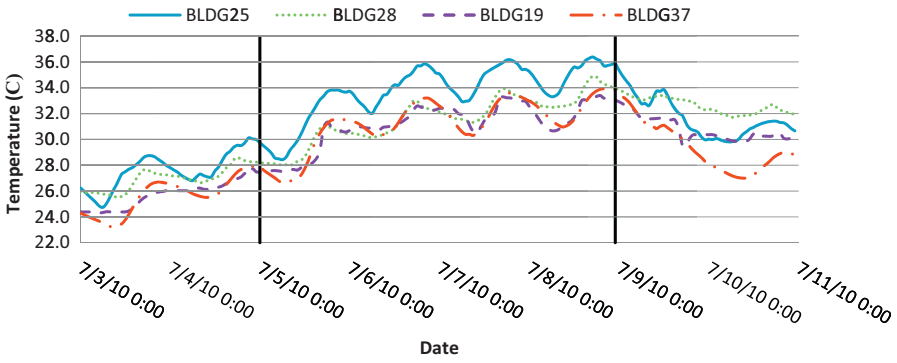

Fig. 2. Measured indoor dry-bulb temperature for Buildings # 25, 28 (BLDG25, BLDG 28 downtown), 19, 37 (BLDG19, BLDG37).

Table 2
Characteristics of the studied buildings.

Segmentation	Height (m)	Aspect ratio	Occupancy (occupant/m^2)	Volume (m^3)	Vegetation ratio	Roof albedo	Envelope albedo	Sensor location
DT – top (a)	20–30	0.95–1.6	Same	12–29 K	Low	0.15	0.25	1
DT – other (b)	20–30	0.95–1.6	Same	12–29 K	Low	0.15	0.25	(0,1)
Other – top (c)	<10	0.18–0.39	Same	<5 K	High	0.15	0.25	1
Other – other (d)	<10	0.18–0.39	Same	<5 K	High	0.15	0.25	(0,1)

Fig. 2 shows measured indoor dry-bulb temperature of one building in downtown (category (a)) and two midrise buildings in category (c) for the period of July 3–10, 2010. It is noteworthy to mention that a heat wave occurred during July 5–8, 2010 (heat wave period is shown within two vertical lines). Building #25 (BLDG25) and Building #28 (BLDG28) are located in the downtown Montreal. It also shows that the hourly measured dry-bulb temperatures (during, before, and after the heat wave) are significantly greater than those of two sample buildings located outside of the downtown areas.

As discussed earlier, the outdoor dry-bulb temperature, the direct normal solar radiation (Sol-Air Model), the wind velocity (wind model), and the relative humidity, were used as the input parameters for both the statistical models. One addition input parameter, the time of the day (0–23) was used for the ANN model. The output of both models was the indoor dry-bulb temperature.

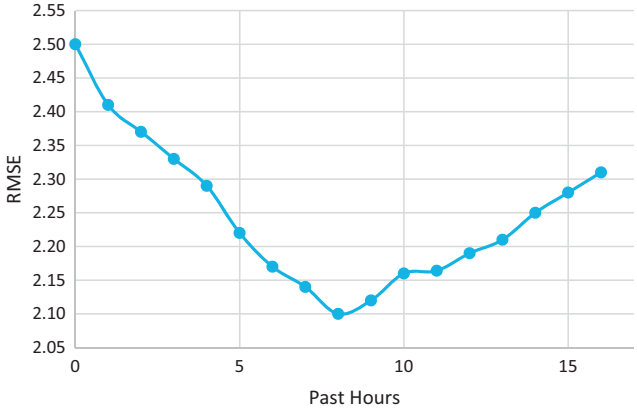

Fig. 3. RMSE of all tested models.

3.3. Time series regression model

The time series model was developed using Analysis ToolPak of Microsoft Excel (2013). The datasets of three units (Building #25, Building #28, and Building #29) located in zone (a), downtown area, corresponding to months June, July, and August 2010 were used to develop the model.

The inputs of the model were the sol-air temperature (°C), wind speed (km/h), and outdoor relative humidity (%). The indoor dry-bulb temperatures of the selected units were considered as the output. The input variables were then increased gradually by adding sol-air temperature of previous hours (up to previous16 h) to find the best model (Fig. 3). To evaluate the model performance, the root mean square error (RMSE) between predicted and actual indoor dry-bulb temperatures was used. The best results were obtained by implementation of the past 8 h observed value of sol-air temperatures (totally 11 inputs). The RMSE of the best model is 2.10 °C. Also, 77% and 86% of the predicted indoor dry-bulb temperatures by this model have an error less than ±2 °C and ±3 °C, respectively. The RMSE for models, including sol-air temperature of 0 h, 4 h, 7 h, 9 h, and 10 h of past time are 2.5 °C, 2.29 °C, 2.14 °C, 2.12 °C, and 2.16 °C, respectively. The following is the obtained equation for this model:

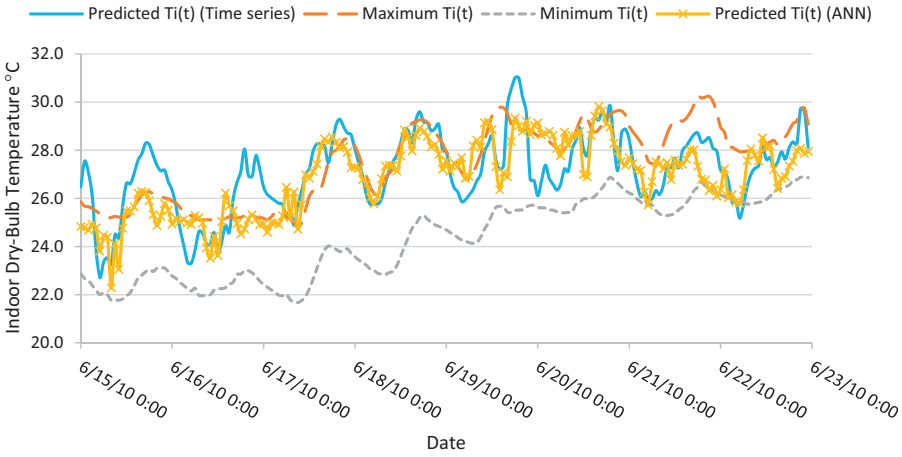

Fig. 4. Simulated hourly indoor dry-bulb temperatures of units in zone (a).

$$T_i(t) = \sum_{k=0}^{8} a_k T_e(t-k) + bW(t) + cRH(t) + d \quad (5)$$

where $T_i(t)$ is the indoor dry-bulb temperature measured at time t. $T_e(t)$ represents the sol-air temperature calculated at time t, based on the outdoor dry-bulb temperature and direct normal solar radiation, $RH(t)$ is the relative humidity, and $W(t)$ is the wind speed.

3.4. Artificial neural networks model

The artificial neural network model was developed using Neural Network Toolbox of MATLAB [39]. The same datasets as the regression approach were used for training the model. A three-layer feed-forward neural network was used to solve the fitting problem between input and output datasets. The network was trained with Levenberg–Marquardt back-propagation algorithm.

The network inputs were the sol-air temperature (°C), wind speed (km/h), outdoor relative humidity (%) and the time of day (0–23). The measured indoor dry-bulb temperatures of the selected units located in the downtown Montreal (Building #25, Building #28, and Building #29) were considered as the desired target of the network. The input datasets were randomly divided up for training, validation and testing stages. 70% of the input datasets (4636 samples) was used at the training stage while the network was adjusted until reaching a minimum error. 15% of the input datasets (994 samples) was used for the validation stage of the network, and for halting the training process when the generalization stopped improving. Finally, the rest of input datasets (994 samples) was used for testing stage. Moreover, the number of hidden neurons was changed from 1 to 100 to achieve the best network performance. Using RMSE between predicted and measured indoor dry-bulb temperatures, the best results were obtained by implementing 10 hidden neurons. The RMSE was 1.76 °C meaning that 75% and 92% of the predicted indoor dry-bulb temperatures had the error of less than ±2 °C and ±3 °C, respectively.

4. Results and discussion

4.1. Cross-comparison of the regression and ANN models in capturing the heat waves

The developed regression and ANN models were used to predict the hourly indoor dry-bulb temperatures of units located in the downtown Montreal (zone (a)). The goal was to determine if the model can accurately predict hourly indoor dry-bulb temperatures. Two samples of datasets were used here by covering a typical summer week (15th to 22nd of June 2010) and the heat wave (5th to 8th of July 2010) in July 2010.

To better evaluate the prediction ability of each model, their output results were compared to corresponding maximum and minimum indoor dry-bulb temperature of datasets related to zone (a). Figs. 4 and 5 show the corresponding measured minimum and maximum indoor dry-bulb temperatures of the three buildings for those periods. Fig. 4 shows simulated indoor dry-bulb temperatures by the time series and ANN models for the period of 15–22 June, 2010 with its corresponding measured maximum and minimum indoor dry-bulb temperatures. The variation of simulated results for time series model about maximum and minimum indoor dry-bulb temperatures are 2.27 °C and 2.31 °C, respectively, for the whole datasets of months June, July, and August 2010. This implies how far the simulated results lie from the maximum and minimum indoor dry-bulb temperatures on average.

The variation of simulated results for ANN model about maximum and minimum indoor dry-bulb temperatures are 1.93 °C and 2.03 °C, respectively, for the same period. This implies how far simulated results lie from the maximum and minimum indoor dry-bulb temperatures on average. It can be seen that the ANN model can accurately predict the indoor dry-bulb temperatures of a typical summer day.

Fig. 5 represents simulated indoor dry-bulb temperatures by the time series and ANN models during the heat wave of July 5–8 2010 (heat wave period is shown within two vertical lines) and its corresponding measured maximum and minimum indoor dry-bulb temperatures. On the contrary of a typical summer day, the time series model was not able to accurately predict the heat wave. However, the ANN model was able to simulate the heat wave. As it is shown, the majority of predicted indoor dry-bulb temperatures by ANN model were more than the minimum indoor dry-bulb temperatures and were very close to the maximum indoor dry-bulb temperatures in that period of the time.

4.2. Cross-comparison of the regression and ANN models in prediction of the heat waves

In this level of simulation, the models were used to simulate hourly indoor dry-bulb temperatures of first eight days of August 2010 when a heat wave occurred on the first three days (heat wave period is shown within two vertical lines). This dataset were not used in the development of the models and thus presents their performance applied on a random buildings. This means that the results were generated based on a totally unknown dataset on this simulation stage.

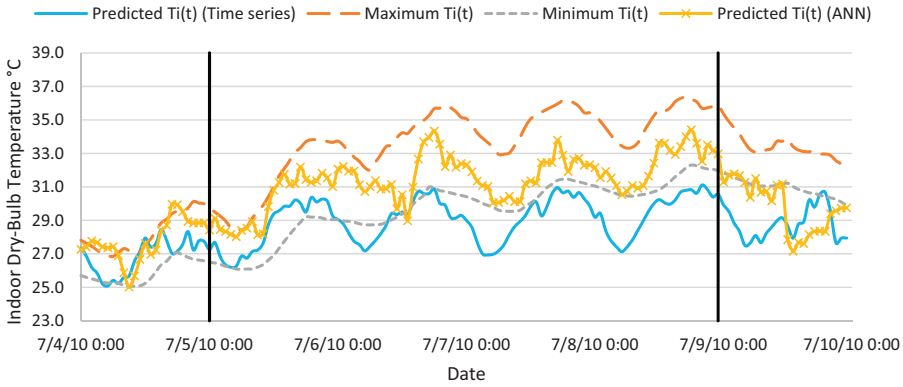

Fig. 5. Simulated hourly indoor dry-bulb temperatures of units in zone (a).

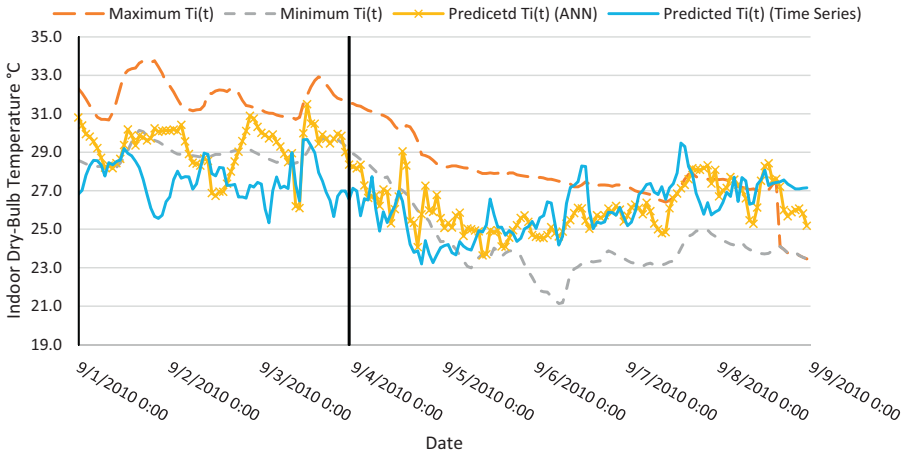

Fig. 6. Predicated results of ANN and time series models correspond to simulation level 2.

The predicted results of the developed models are illustrated in Fig. 6. The variation of time series model about measured maximum and minimum indoor dry-bulb temperatures are 3.39 °C and 2.23 °C, respectively. But again, the ANN model shows better performance in predicting the indoor dry-bulb temperature comparing to the time series model. The variation of predicted results of ANN model about maximum and minimum indoor dry-bulb temperatures are 2.64 °C and 1.99 °C, respectively.

An important observation from Fig. 6 and also by considering the discussed results above is that the predictions made by the ANN model are still closer to the maximum indoor dry-bulb temperatures, reinforcing the use of this model to assess the worst case scenarios of indoor dry-bulb temperatures prediction.

As it was shown before, the difference between predicted results by any of two models and the corresponding maximum indoor dry-bulb temperature was increased during the heat waves. The reason can be explained as the limited number of days in heat waves that was used to develop models (July 5–8, 2010). Also, all the generalizations that were discussed in Section 3.2 can play a role in decreasing the accuracy of the predicted results especially during the heat waves.

5. Conclusion

In this study, the existing measured data were used to develop predictive tools to characterize the relationship between indoor dry-bulb temperatures and outdoor thermal conditions of the worst case scenario during the heat waves. For this purpose, different building characteristic and environmental parameters were analyzed.

For the time series model, although it requires more input, the simulations give larger error compare to the ANN model. The ANN model needs more expertise compare to the time series model. Moreover, developing and finding the best fit line for the ANN model is more time consuming. However, the advantages of this model greatly outweigh its drawbacks and prediction results accuracy is noticeably increased by using this model. The good agreement between the prediction made by the ANN model and the measured data clearly demonstrated its capability of approximating nonlinear relations even in a complex situation where some important influential parameters are unclear.

Acknowledgments

The authors would like to express their gratitude to Institut national de santé publique du Québec (INSPQ) Ouranos and The Climate Change and Health Office of Health Canada for their support.

References

[1] P.A. Mirzaei, F. Haghighat, Approaches to study urban heat island – abilities and limitations, Building and Environment 45 (10) (2010) 2192–2201.
[2] M. Kolokotroni, X. Ren, M. Davies, A. Mavrogianni, London's urban heat island: impact on current and future energy consumption in office buildings, Energy and Buildings 47 (April) (2012) 302–311.
[3] T.R. Oke, C. East, The urban boundary layer in Montreal, Boundary-Layer Meteorology 1 (4) (1971) 411–437.

[4] C. Estournel, R. Vehil, D. Guedalia, J. Fontan, A. Druilhet, Observations and modeling of downward radiative fluxes (solar and infrared) in urban/rural areas, Journal of Climate and Applied Meteorology 22 (1) (1983) 134–142.
[5] M. Zinzi, S. Agnoli, Cool and green roofs. An energy and comfort comparison between passive cooling and mitigation urban heat island techniques for residential buildings in the Mediterranean region, Energy and Buildings 55 (December) (2012) 66–76.
[6] T.R. Oke, R.A. Spronken-Smith, E. Jauregui, C.S. Grimmond, The energy balance of central Mexico City during the dry season, Atmospheric Environment 33 (24) (1999) 3919–3930.
[7] R. Bornstein, Q. Lin, Urban heat islands and summertime convective thunderstorms in Atlanta: three case studies, Atmospheric Environment 34 (3) (2000) 507–516.
[8] R. Giridharan, S.S.Y. Lau, S. Ganesan, Nocturnal heat island effect in urban residential developments of Hong Kong, Energy and Buildings 37 (September (9)) (2005) 964–971.
[9] S. Hajat, R.S. Kovats, R.W. Atkinson, A. Haines, Impact of hot temperatures on death in London: a time series approach, Journal of Epidemiology and Community Health 56 (5) (2002) 367–372.
[10] O. Wilhelmi, K. Purvis, R. HarissPurvis, Designing a geospatial information infrastructure for mitigation of heat wave hazards in urban areas, Natural Hazards Review (2004) 147–158.
[11] A. Mavrogianni, P. Wilkinson, M. Davies, P. Biddulph, E. Oikonomou, Building characteristics as determinants of propensity to high indoor summer temperatures in London dwellings, Building and Environment 55 (2012) 117–130.
[12] S. Hajat, R. Kovats, K. Lachowycz, Heat-related and cold-related deaths in England and Wales: who is at risk? Occupational and Environmental Medicine 64 (2) (2007) 93–100.
[13] UKCIP, Climate digest, 2010, September, Retrieved from http://www.ukcip.org.uk/climate-digest/
[14] R. Pachauri, A. Reisinger, Contribution of Working Groups I, II and III to the Fourth Assessment Report of the Intergovernmental Panel on Climate Change, Geneva, Switzerland, 2007.
[15] L.S. Kalkstein, P.F. Jamason, J.S. Greene, J. Libby, L. Robinson, The Philadelphia hot weather-health watch/warning system: development and application, Bulletin of the American Meteorological Society 77 (7) (1996) 1519–1528.
[16] NOAA, Regional Operations Manual Letter, Eastern Region National Weather Service, Bohemia, NY, 1994.
[17] E. Oikonomou, M. Davies, A. Mavrogianni, P. Biddulph, P. Wilkinson, M. Kolokotroni, Modelling the relative importance of the urban heat island and the thermal quality of dwellings for overheating in London, Building and Environment 57 (2012) 223–238.
[18] P. Lankester, P. Brimblecombe, Future thermohygrometric climate within historic houses, Journal of Cultural Heritage 13 (1) (2012) 1–6.
[19] L. Guan, Energy use, indoor temperature and possible adaptation strategies for air-conditioned office buildings in face of global warming, Building and Environment 55 (2012) 8–19.
[20] ASHRAE Handbook – Fundamentals, American Society of Heating, Refrigerating and Air-Conditioning Engineers, Inc., Atlanta, GA, 2009.
[21] L. Zhou, F. Haghighat, Optimization of ventilation system design and operation in office environment. Part I: Methodology, Building and Environment 44 (2009) 651–656.
[22] J. Zhang, F. Haghighat, Development of artificial neural network based heat convection algorithm for thermal simulation of large rectangular cross-sectional area earth-to-air heat exchangers, Energy and Buildings 42 (2010) 435–440.
[23] L. Magnier, F. Haghighat, Multiobjective optimization of building design using TRNSYS simulations, genetic algorithm, and artificial neural network, Building and Environment 45 (2010) 739–746.
[24] A. Bastani, F. Haghighat, J. Kozinski, Contaminant source identification within a building: toward design of immune buildings, Building and Environment 51 (2012) 320–329.
[25] A. El-Sawi, F. Haghighat, H. Akbari, Assessing long-term performance of centralized thermal energy storage system, Applied Thermal Engineering 62 (2014) 313–321.
[26] B. Thomas, M. Soleimani-Mohseni, Artificial neural network models for indoor temperature prediction: investigations in two buildings, Neural Computing & Applications 16 (1) (2007) 81–89.
[27] T. Lu, M. Viljanen, Prediction of indoor temperature and relative humidity using neural network models: model comparison, Neural Computing & Applications 18 (4) (2009) 345–357.
[28] K.W. Park, H. Akbari, F. Haghighat, Measuring, Modeling Indoor Thermal Conditions in Urban Heat Island Areas: The Case of Montreal Island, Montreal, 2010.
[29] V. Bonacquisti, G. Casale, S. Palmieri, A. Siani, A canopy layer model and its application to Rome, Science of the Total Environment 364 (1) (2006) 1–13.
[30] P. Mirzaei, F. Haghighat, A. Nakhaie, A. Yagouti, R. Keusseyan, A. Coman, Indoor thermal condition in urban heat island – development of a predictive tool, Building and Environment 57 (2012) 7–17.
[31] N.B. Hutcheon, G.O. Handegord, Building Science for a Cold Climate, Wiley, 1983.
[32] C.Y. Lam, On climate changes brought about by urban living, PGBC Symposium, 2 December, Hong Kong, China, 2006.
[33] D. Sailor, N. Dietsch, The urban heat island mitigation impact screening tool (MIST), Environmental Modelling & Software 22 (10) (2007) 1529–1541.
[34] R. Giridharan, S. Lau, S. Ganesan, B. Givoni, Urban design factors influencing heat island intensity in high-rise high-density environments of Hong Kong, Building and Environment 42 (10) (2007) 3669–3684.
[35] K. Gobakis, D. Kolokotsa, A. Synnefa, M. Saliari, K. Giannopoulou, M. Santamouris, Development of a model for urban heat island prediction using neural network techniques, Sustainable Cities and Society 1 (2011) 104–115.
[36] M. Barrow, K. Clark, Heat-related illnesses, American Family Physician 58 (3) (1998) 749.
[37] L. Shashua-Bar, M. Hoffman, Y. Tzamir, Integrated thermal effects of generic built forms and vegetation on the UCL microclimate, Building and Environment 41 (3) (2006) 343–354.
[38] A. Wright, A. Young, S. Natarajan, Dwelling temperatures and comfort during the August 2003 heat wave, Building Services Engineering Research and Technology 26 (2005) 285–300.
[39] MATLAB, R2012b Math Works Documentation, Math Work Inc, 2012.